SAJSET
ISSN: 2992-3581

Savannah Journal of Science and Engineering Technology
Volume: 01; Issue: 04; Pages: 195-201; 2023.
www.sajsetjournal.com.ng

DOI: xx.xxxx.x/sajset-01-2023-0044

SAJSET
ISSN: 2992-3581

Determination of optimum combination for CuO/CeO_5 oxygen carriers in the production of syngas using chemical looping

Saddiq, H. A., Abubakar, M. A., Waziri, A. Y. and Abubakar, H.
Department of Chemical Engineering, Modibbo Adama University, Girei Road, Yola, Adamawa State, 652105, Nigeria

Paper History
Received: 01st June, 2023
Accepted: 6th August, 2023
Published: August, 2023

Corresponding author
Saddiq, H. A.
kabsaddiq@mau.edu.ng

Abstract:
Synthesis gas is a gaseous fuel that is composed of carbon II oxide (CO) and hydrogen (H_2) which can be produced from various fuel either in gaseous, liquid or solid form with the gaseous fuel being the most predominant. There are various conventional means of producing syngas among which is chemical looping where metal oxides called oxygen carriers are used for transferring both material and energy between two or more reactors thereby interloping both exothermic and endothermic reactions in a cyclic form. CuO is one of the oxides with oxygen uncoupling characteristics, so it is very reactive and can be used to modify other metal oxides such as CeO_2. It has been shown that CuO/CeO_2 is a good material for production of syngas but their optimum combination has not been reported. This study therefore wishes to determine the optimum combination of CuO and CeO_2 to form a composite of CuO/CeO_2 oxygen carrier that gives the best desirability in terms of reactivity, selectivity and stability in the production of syngas. This is done by using liquefied petroleum gas (LPG) as fuel at a temperature of 800°C. The oxygen carrier material was synthesized using coprecipitation method and then used in a fixed bed reactor for the study. Response surface methodology (RSM) in Design expert 6.0.6 was used for the optimization. It was discovered that 10% CuO composition was found to be the optimum value in term of reactivity, syngas selectivity as well as stability of the material, with desirability of 84.9%. The reactivity obtained for that combination was found to be 67.67% while the CO selectivity, H_2 selectivity and degradation are found to be 84.28%, 91.11% and 3.56% respectively.

Keywords: *Cerium oxide, Chemical looping, Optimization, Oxygen carrier, Syngas*

1. Introduction

Syngas is a gaseous fuel comprising H_2 and CO as the major components [1]. It can be manufactured through a chemical reaction in which hydrocarbon molecules in the feedstock such as natural gas, Liquefied Petroleum Gas (LPG) and other solid and gaseous fuels are broken down by the introduction of oxygen (via air or steam) to produce hydrogen and carbon monoxide [24]. LPG can be obtained as a bye product during the processing of natural gas by removing excess propane and butane [2] or from distillation process of petroleum refining [3]. It is mainly composed of propane and butane and exists in liquid form at ambient temperature and moderate pressure of less than 1.5 MPa. LPG has a boiling point ranging between -44°C to 0°C and ignition temperature of around 482°C [3]. Chemical looping technology is a technology that involves the continuous circulation of oxygen carrier between the fuel reactor (FR) and the air reactor (AR) for its oxidation and reduction [4]. They are of two types; chemical looping combustion where complete combustion of the fuel to yield CO_2 and H_2O is achieved and chemical looping reforming where partial oxidation of the fuel to yield CO and H_2 is achieved [5]. The diagram for chemical looping reforming is illustrated in Figure. 1.

The various reactions involved as adopted from [6] are:

$$\mathrm{MeO}_x(s) + \frac{1}{2}O_2(g) \leftrightarrow MeO_{(x+1)}(s) \quad \Delta H = -ve \tag{1}$$

$$C_nH_{2m}(g) + nMeO_{(x+1)}(s) \leftrightarrow \mathrm{n}CO(g) + mH_2(g) + nMeO_x(s)\Delta H = +ve \tag{2}$$

$$MO(s) + CO_2(g) \leftrightarrow \mathrm{M}CO_3(s)\,\Delta H = -ve \tag{3}$$

$$MCO_3(s) \leftrightarrow \mathrm{M}O(s) + CO_2(g)\ \Delta H = +ve \tag{4}$$

Many works on syngas production have reported that utilization of CeO_2 in combination with other metal oxides such as CuO, Mn_2NO_5, Fe_2O_5 as oxygen carriers gives high selectivity to syngas but it is associated with the problem of poor stability at high temperature of above 850°C and low reactivity at low temperature of less than 800°C [7, 8]. Even though it has been reported that combination of CuO and CeO_2 as oxygen carriers can yield syngas, the optimum combination has not been reported

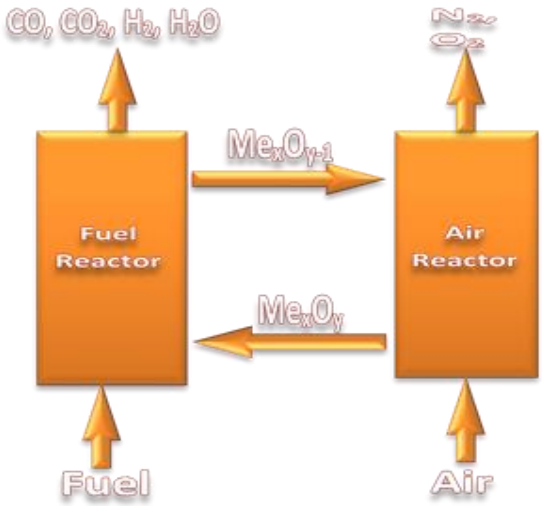

Figure 1: Demonstrating Chemical Looping Reforming

Response surface methodology (RSM) embedded in Design expert 6.0.6 is an optimization tool that can be used to determine optimum phenomena by analysing various input and responses. The validity of the models used to obtain the optimum combination from design expert can be analysed using ANOVA. The F and P values of the 'model' and those of 'lack of fit' give an insight as regards the validity for use of the selected models [9, 10] while the Adj. R^2, Pred. R^2 and the adequate precision confirms the validity of their use. The model is considered to be valid if the data fits the model which can be seen from higher model F values and lower 'lack of fit' values [11]. The extent of their size is determined by the P values which are expected to be less than 0.05 [12]. The validity of the models can be confirmed by maximizing the adjusted R^2, the predicted R^2 and the adequate precision. The difference between the predicted and adjusted R^2 is expected to be less than 20% for the model to be valid while the adequate precision is expected to be greater than 4 [11].

This research prepares oxygen carriers using different combination ratios of CuO and CeO_2 which is used in the production of synthesis gas using LPG as fuel, with the aim of determining the optimum combination of the two oxides.

2. Materials and Methods

2.1 Oxygen carrier preparation

For the preparation of composite of CuO and CeO_2, Copper (II) nitrate trihydrate ($Cu(NO_3)_2.3H_2O$) and cerium (IV) nitrate hexahydrate ($Ce(NO_3)_3.6H_2O$) are dissolved in distilled water and then heated to a temperature of 80°C while stirring vigorously. Ammonium hydroxide (NH_4OH) is then added to achieve pH of 8.0 to 9.5 to form precipitate and it is then maintained at that temperature and stirring for further two hours to aid aging. The precipitate is then filtered and washed with deionized water after which it is dried in an oven at a temperature of 110°C for 5 hours. It is then crushed to powder form and calcined at a temperature of 600°C for 2 hours and then at a temperature of 900°C for further 3 hours to obtain the oxygen carrier.

2.2 Experimental procedure

The experiment was carried out using a fixed bed reactor setup situated at the mini refinery of ABU Zaria and the process flow diagram of the setup is shown in Figure 2.

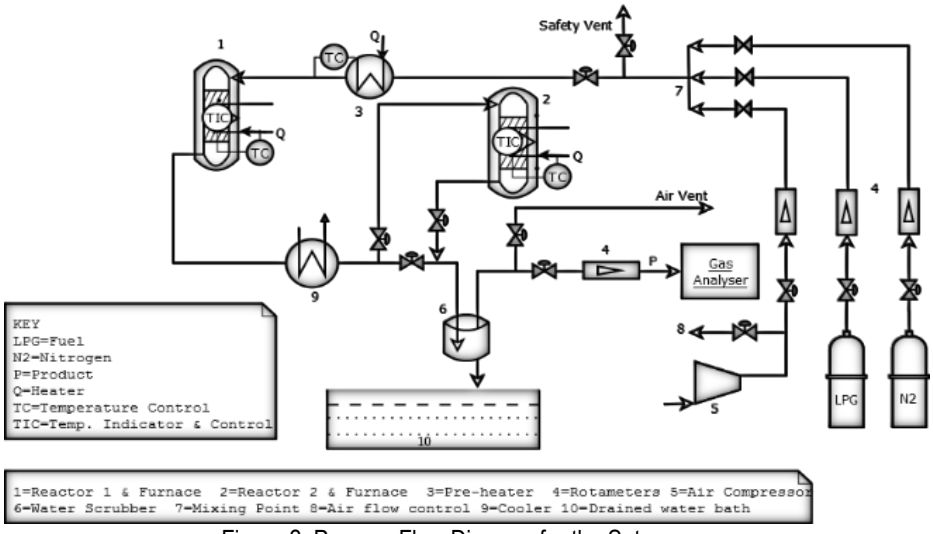

Figure 2: Process Flow Diagram for the Setup

Three grams of the oxygen carrier is loaded into reactor supported on coarse sand (SiO_2) and glass wool both below and above the oxide bed. The furnace is then switched on so as to heat up the reactor bed to the required temperature of 800°C where oxidation of the metal/metal oxide takes place for five minutes after which nitrogen is passed through the reactor for five minutes so as to create inert atmosphere for the subsequent reaction. Air is then allowed to flow to the reactor at a flow rate of 200 ml/min for five minutes for the oxidation of the oxygen carrier after which nitrogen is again allowed to flow to the reactor at the rate of 300 ml/min for about five minutes before switching on the flow of LPG at a flow rate of 100 ml/min flowing together with nitrogen at 200 ml/min for five minutes which completes one cycle. The product gas after the first and twentieth cycles are collected in gas bags to determine the composition of the products using gas analyser.

2.3 Reactions involved in chemical looping

The reactions of one mole for each of the components in the fuel with the oxygen carrier for complete combustion and partial oxidation are as adopted from [13–15] given here;

$$C_3H_8 + 3Me_xO_y \rightarrow 3CO + 4H_2 + 3Me_xO_{y-1} \quad (5)$$

$$C_4H_{10} + 4Me_xO_y \rightarrow 4CO + 5H_2 + 4Me_xO_{y-1} \quad (6)$$

$$C_3H_8 + 5Me_xO_y \rightarrow 3CO_2 + 4H_2O + 5Me_xO_{y-2} \quad (7)$$

$$C_4H_{10} + \tfrac{13}{2}Me_xO_y \rightarrow 4CO_2 + 5H_2O + \tfrac{13}{2}Me_xO_{y-2} \quad (8)$$

The conversion of the fuel can be determined by using the expression

$$x = \frac{Fuel\ in - fuel\ out}{fuel\ in} \times 100\% \quad (9)$$

3 Results and Discussions

3.1 Characterisation

The XRD spectra of the oxides for some selected percentages of CuO loading were cascaded and presented in Figure. 3.

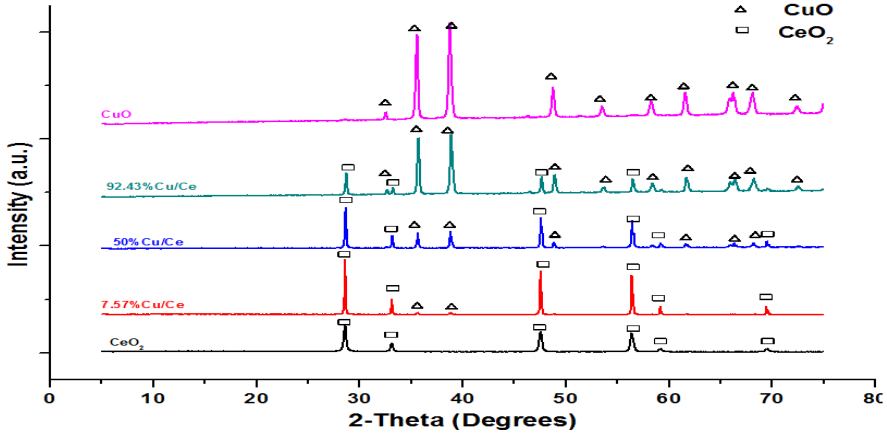

Figure 3: XRD spectra for CuO/CeO_2 with Different Percentages of CuO as Shown

From Figure 3, it can be observed that crystal peaks corresponding to CuO and CeO_2 are shown at the 2θ positions of 36, 38 48 and 68 for CuO and 28, 34, 47 and 56 for CeO_2 as presented by researchers such as [16–18] where CuO peaks intensity increases with increase in CuO loading. The sharpness of the peaks indicates that the materials are crystalline in nature as reported by [16] that when calcined at low temperature, the peaks were observed to be diffused because crystals are only formed when calcined at higher temperature. Further observation of Figure. 3 shows that there are no other peaks present apart from those reflected from either CuO or CeO_2 whose XRD are presented as single materials which is an indication that there was no interaction between the two materials for the formation of other compounds. The fuel (LPG) was analysed using GC-MS and it was found to contain 16.445% propane (C_3H_8) and 83.555% butane (C_4H_{10}).

3.2 Experimental Results

After the experiment, the responses are obtained and presented as shown in Table 1.

From Table 1, it can be observed that there are two values of each response i.e the conversion, selectivity and the degradation presented for each oxygen carrier. The first value represents the data obtained after the first cycle of operation while the second value represents the value obtained after the 20th cycle of operation. This is done to determine the extent of degradation of the oxygen carrier after long time operation as one of the criteria for determining the quality of oxygen carrier [19, 20]. This is done by calculating the percentage difference between the reactivity of the first cycle and that of the 20th cycle. The table shows that there are instances where the reactivity after 20th cycle is higher than that after first cycle. This is an indication that some materials become more active as it is continually used for the reaction [21].

3.3 Optimization results

The ANOVA table result for the analysis is shown in Table 2 where F is the fit value, P is the probability of fittings, R^2 is the regression coefficient, Adj. is adjusted values, Pred. is the predicted value, Adeq. Prec. Is the adequate precision.

Table 1: Conversion and Selectivity of the Products from the Reaction for CuO/CeO_2

S/No	Trial	% of CuO in CuO/CeO_2	Mole Composition			Conv. (%)	Selectivity (%)			Degr. (%)
			CO	CO_2	H_2		CO	CO_2	H_2	
1	1	92.45 Cu/Ce	0.001206	0.002520	0.000000	11.33	32.37	67.63	0.00	11.272
			0.001129	0.001986	0.001197	10.06	36.24	63.76	11.15	
2	1	80.00 Cu/Ce	0.002608	0.002356	0.000000	10.60	52.54	47.46	0.00	0.000
			0.001864	0.002242	0.002394	12.33	45.40	54.60	18.19	
3	1	50.00 Cu/Ce	0.004515	0.001333	0.000000	6.00	77.20	22.80	0.00	0.000
			0.004233	0.001170	0.000000	5.26	78.35	21.65	0.00	
4	1	20.00 Cu/Ce	0.003121	0.000316	0.015563	16.00	90.82	9.18	91.12	0.000
			0.003617	0.000245	0.018676	18.59	93.66	6.34	94.08	
5	1	7.57 Cu/Ce	0.007029	0.002634	0.070394	77.78	72.74	27.26	84.77	1.328
			0.007269	0.002155	0.071591	76.75	77.13	22.87	87.37	
6	2	92.43 Cu/Ce	0.001796	0.002095	0.000000	9.42	46.15	53.85	0.00	0.000
			0.001385	0.002318	0.000838	11.21	37.41	62.59	7.00	
7	2	50.00 Cu/Ce	0.004626	0.001616	0.001437	8.62	74.11	25.89	15.62	0.000
			0.004549	0.002046	0.005148	14.03	68.98	31.02	34.38	
8	2	7.57 Cu/Ce	0.007816	0.001736	0.077457	80.36	81.83	18.17	90.28	0.000
			0.007653	0.001442	0.087513	88.46	84.15	15.85	92.67	

Table 2: ANOVA Table for CuO/CeO_2 Oxygen Carrier Optimization

Response	Model	Model		Lack of Fit		R^2	Adj. R^2	Pred. R^2	Adeq. Prec
		F	P	F	P				
Reactivity	CBC	28.74	0.0036	8.45	0.0622	0.9557	0.9224	0.7529	11.575
CO Select.	CBC	57.92	0.0009	0.97	0.3981	0.9775	0.9606	0.9106	17.133
H_2 Select.	QRC	17.18	0.0058	2.19	0.2588	0.8730	0.8222	0.6984	8.237
Degrad.	QRC	1.09	0.4048	0.17	0.8529	-	-	-	2.305

From Table 2, it can be observed that CBC model was selected for both reactivity and CO selectivity while QRC model was selected for both H_2 selectivity and degradation. The model P values are all below 0.05 for the selected models, save for degradation which is around 0.0622 which is an indication that the selected models are valid and the data will accurately fit the models.

To confirm the validity of the model, it can be observed from the table that the differences between the adjusted and predicted R^2 values are less than 20%. Large values of adequate precision can also be observed from the table with most of the values being above 4, recommended for validity of model [12]. It is therefore reasonable to conclude that the selected models are adequate for use in the analyses of the optimum CuO loading for this process. The models can further be validated by normal plots of the residuals for various responses as shown in Figure 4.

From Figure. 4, it can be observed that the data points of the residuals for all the responses are evenly distributed around the model line, which is an indication that there are minimal errors in using the selected models.

The selected models were then used with the responses obtained from laboratory analyses to determine the CuO loading between the values of 10% and 90% that will yield best desirability in terms of the responses. The numerical optimization settings is as presented in Table 3 while the numerical optimization results is shown in Table 4.

Table 3: Numerical Optimization Settings for CuO/CeO_2

Constraints Name	Goal	Lower Limit	Upper Limit	Importance
CuO Load	Is in range	10	90	3
Reactivity (%)	Maximize	0	100	3
CO Selectivity (%)	Maximize	0	100	3
H_2 Selectivity (%)	Maximize	0	100	3
Degradation (%)	Minimize	0	100	3

Table 4: Numerical Optimum Result for CuO/CeO_2

Solutions						
No	CuO Load	Reactivity (%)	CO Selectivity. (%)	H_2 Selectivity. (%)	Degradation (%)	Desirability
*1	10.00	67.67	84.28	91.11	3.56	0.849
2	61.80	14.46	60.88	15.68	9.65	0.292

* Selected

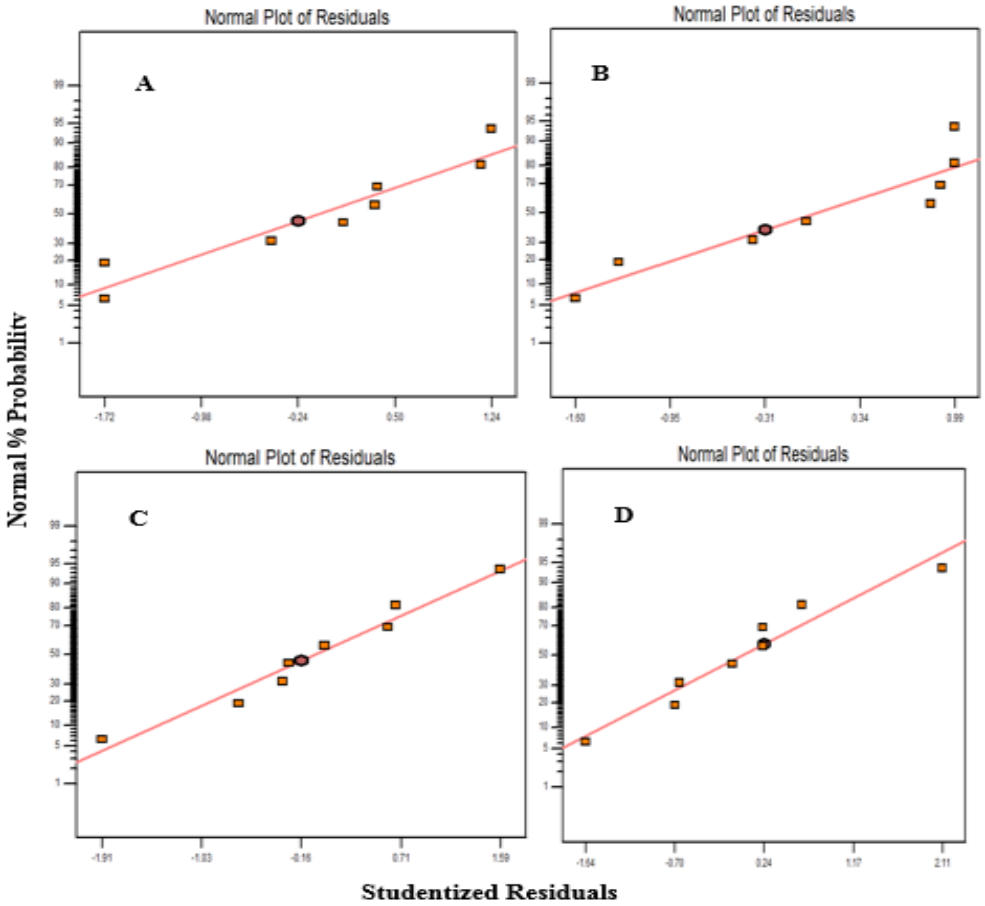

Figure 4: Normal Plot of Residuals for CuO/CeO$_2$ Oxygen Carrier (A) Reactivity (B) CO Selectivity (C) H$_2$ Selectivity (D) Degradation

From the results obtained in Table 4, it can be observed that the CuO loading with the maximum desirability is that with 10% loading with desirability of 84.9%. The reactivity obtained for that loading was found to be 67.67% while the CO selectivity, H_2 selectivity and degradation are found to be 84.28%, 91.11% and 3.56% respectively. Since our desire is to have a sample with high selectivity to syngas without compromising high reactivity and low degradation of the material, these values obtained here is found to be the best from the data analysed. It will therefore be reasonable to conclude that the material with 10% CuO loading is expected to give the best outcome for the desired reaction under study.

To validate the model prediction, 10% CuO loading was synthesized for each of the oxygen carriers and experiments were performed for validation as shown in Table 5.

Table 5: Comparison between the experimental result and the predicted model

	Model	Experimental	Variation
Reactivity	67.6700	68.4500	0.6700
H_2 Selectivity	84.2800	84.0700	0.2100
CO Selectivity	91.1100	88.1400	2.9700
Degradation	3.5600	3.5600	0.0000

From Table 5, there is agreement between the experimental result and the model with little disparity which is an indication that the model gave accurate prediction of the system thereby confirming that the 10% CuO loading predicted is the actual optimum for the system.

The morphology of the oxygen carriers with 10 % CuO loading for both fresh material and material after 15 cycles were investigated using scanning electron microscope (SEM) and the images for CuO/CeO$_2$ oxygen carrier is shown in Plate I.

From Plate I, it can be observed that the material is made of granular surfaces in sizes ranging from less than 1 µm to around 50 µm which shows that the particles can be described as having microsize. Observing the two images in Plate I, it can be seen that there is no significance difference between the fresh oxygen carrier and oxygen carrier after 15 cycles of operation which is an indication that there is no degradation of the material in term of their structure. This means that the material can be used for a long period of time without significance change in the reactivity of the material.

The physical properties of oxygen carriers with 10% CuO content are presented in Table 6.

Table 6: Physical Properties of CuO/CeO$_2$ Oxygen Carriers

Oxygen Carrier	Pore Volume (cm^3/g)	Pore Size (nm)	BET Surface Area (m^2/g)
CuO/CeO$_2$	0.0810	2.647	251.5

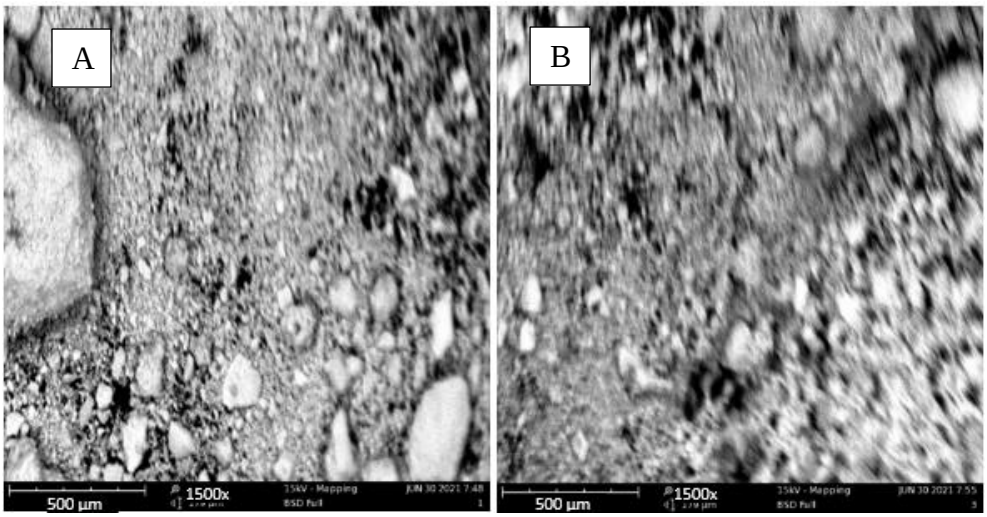

Plate I: SEM Images of Oxygen Carrier with 10 % CuO for fresh CuO/CeO_2 oxygen carrier (A) and CuO/CeO_2 Oxygen Carrier after 15 cycles (B) with 1500x Magnification

From Table 6, it can be observed that the BET surface areas of the two oxygen carriers are much higher when compared to those of single particles which are reported to be 79.50 m^2/g for Nb_2O_5 [22] and 131.1 m^2/g for CeO_2 [23] which is an indication that there is an improvement in the surface area of the oxygen carriers when CuO is added to the individual materials. These show that when CuO is added to the individual oxygen carriers, the surface needed for the reaction of the fuel are increased which means that the reactivity of the materials is expected to increase compared to those without the addition of CuO. The pore sizes of the oxygen carriers are 2.647 nm.

4 Conclusion

The CuO/CeO_2 oxygen carriers prepared are found to be crystalline in nature with high XRD intensity peaks and the oxygen carrier with 10% CuO composition is granular in nature with CuO/CeO_2 having grains of 1 to 50 µm and high BET surface for reaction having surface area of 325.4 m^2/g. Oxygen carrier with 10% CuO composition gives the best desirability of 84.9% for CuO/CeO_2 in terms of syngas selectivity, reactivity and stability at 800^{o}C in both oxygen carriers and the physical feature shows that CuO/CeO_2 oxygen carrier is stable after long usage as evident from their SEM images before and after 15 cycles of operations.

Acknowledgement

The author are very grateful to Petroleum Technology Development Fund (PTDF), Nigeria for providing the fund needed to carry out this research work.

References

[1]. Iaquaniello, G., Antonetti, E., Cucchiella, B., Palo, E., Salladini, A., Guarinoni, A., Basini, L. (2012). Natural Gas Catalytic Partial Oxidation: A Way to Syngas and Bulk Chemicals Production. In S. Gupta (Ed.), *Natural Gas - Extraction to End Use*. InTech. https://doi.org/10.5772/48708

[2]. Malaibari, Z. (2011). *Hydrogen Production from Liquefied Petroleum Gas (LPG) by Oxidative Steam Reforming Over Bimetallic Catalysts* (Doctor of Philosophy). University of Waterloo, Ontario, Canada.

[3]. Lu, C., Li, K., Wang, H., Zhu, X., Wei, Y., Zheng, M., & Zeng, C. (2018). Chemical looping reforming of methane using magnetite as oxygen carrier: Structure evolution and reduction kinetics. *Applied Energy*, *211*, 1–14. https://doi.org/10.1016/j.apenergy.2017.11.049

[4]. Ghoneim, S. A., El-Salamony, R. A., & El-Temtamy, S. A. (2016). Review on Innovative Catalytic Reforming of Natural Gas to Syngas. *World Journal of Engineering and Technology*, *04*(01), 116–139. https://doi.org/10.4236/wjet.2016.41011

[5]. Li, F., Zeng, L., Velazquez-Vargas, L. G., Yoscovits, Z., & Fan, L.-S. (2010). Syngas chemical looping gasification process: Bench-scale studies and reactor simulations. *AIChE Journal*, *56*(8), 2186–2199. https://doi.org/10.1002/aic.12093

[6]. Matzen, M., Pinkerton, J., Wang, X., & Demirel, Y. (2017). Use of natural ores as oxygen carriers in chemical looping combustion: A review. *International Journal of Greenhouse Gas Control*, *65*, 1–14. https://doi.org/10.1016/j.ijggc.2017.08.008

[7]. Bhavsar, S., & Veser, G. (2014). Chemical looping beyond combustion: production of synthesis gas via chemical looping partial oxidation of methane. *RSC Adv.*, *4*, 47254–47267. https://doi.org/10.1039/C4RA06437B

[8]. Nasr, S. (2012). *The reduction kinetics of iron oxide ore by methane for chemical-looping combustion* (Masters). Dalhousie University Halifax, Nova Scotia.

[9]. Hambali, H. U., Jalil, A. A., Abdulrasheed, A. A., Siang, T. J., Owgi, A. H. K., & Aziz, F. F. A. (2021). CO2 reforming of methane over Ta-promoted Ni/ZSM-5 fibre-like catalyst: Insights on deactivation behavior and optimization using response surface methodology (RSM). *Chemical Engineering Science*, *231*, 116320.

https://doi.org/10.1016/j.ces.2020.116320

[10]. Shahbaz, M., Yusup, S., Inayat, A., Patrick, D. O., Pratama, A., & Ammar, M. (2017). Optimization of hydrogen and syngas production from PKS gasification by using coal bottom ash. *Bioresource Technology*, *241*, 284–295. https://doi.org/10.1016/j.biortech.2017.05.119

[11]. Noordin, M. Y., Venkatesh, V. C., Sharif, S., Elting, S., & Abdullah, A. (2004). Application of response surface methodology in describing the performance of coated carbide tools when turning AISI 1045 steel. *Journal of Materials Processing Technology*, *149*, 46–58. https://doi.org/10.1016/S0924-0136(03)00861-6

[12]. Forutan, H. R., Karimi, E., Hafizi, A., Rahimpour, M. R., & Keshavarz, P. (2015). Expert representation chemical looping reforming: A comparative study of Fe, Mn, Co and Cu as oxygen carriers supported on Al_2O_3. *Journal of Industrial and Engineering Chemistry*, *21*, 900–911. https://doi.org/10.1016/j.jiec.2014.04.031

[13]. Adanez, J., Abad, A., Garcia-Labiano, F., Gayan, P., & de Diego, L. F. (2012). Progress in Chemical-Looping Combustion and Reforming technologies. *Progress in Energy and Combustion Science*, *38*(2), 215–282. https://doi.org/10.1016/j.pecs.2011.09.001

[14]. Cheng, Z., Qin, L., Fan, J. A., & Fan, L.-S. (2018). New Insight into the Development of Oxygen Carrier Materials for Chemical Looping Systems. *Engineering*, *4*(3), 343–351. https://doi.org/10.1016/j.eng.2018.05.002

[15]. Go, K., Son, S., & Kim, S. (2008). Reaction kinetics of reduction and oxidation of metal oxides for hydrogen production. *International Journal of Hydrogen Energy*, *33*(21), 5986–5995. https://doi.org/10.1016/j.ijhydene.2008.05.039

[16]. Djinović, P., Batista, J., & Pintar, A. (2008). Calcination temperature and CuO loading dependence on CuO-CeO2 catalyst activity for water-gas shift reaction. *Applied Catalysis A: General*, *347*(1), 23–33. https://doi.org/10.1016/j.apcata.2008.05.027

[17]. Ferreira, A. C., Ferraria, A. M., do Rego, A. M. B., Gonçalves, A. P., Girão, A. V., Correia, R., … Branco, J. B. (2010). Partial oxidation of methane over bimetallic copper–cerium oxide catalysts. *Journal of Molecular Catalysis A: Chemical*, *320*(1–2), 47–55. https://doi.org/10.1016/j.molcata.2009.12.014

[18]. Lu, C., Deng, R., Xu, R., Zhao, Y., Zhu, X., Wei, Y., & Li, K. (2021). Design of hybrid oxygen carriers with CeO2 particles on MnCo2O4 microspheres for chemical looping combustion. *Chemical Engineering Journal*, *404*, 126554. https://doi.org/10.1016/j.cej.2020.126554

[19]. Cho, P. (2005). *Development and characterisation of oxygen-carrier materials for chemical-looping combustion*. Göteborg: Chalmers Univ. of Technology.

[20]. Adánez-Rubio, I., Pérez-Astray, A., Abad, A., Gayán, P., De Diego, L. F., & Adánez, J. (2019). Chemical looping with oxygen uncoupling: an advanced biomass combustion technology to avoid CO2 emissions. *Mitigation and Adaptation Strategies for Global Change*, *24*(7), 1293–1306. https://doi.org/10.1007/s11027-019-9840-5

[21]. Dai, J., & Whitty, K. J. (2019). Predicting and alleviating coal ash-induced deactivation of CuO as an oxygen carrier for chemical looping with oxygen uncoupling. *Fuel*, *241*, 1214–1222. https://doi.org/10.1016/j.fuel.2019.02.029

[22]. Raba, A. M., Bautista-Ruíz, J., & Joya, M. R. (2016). Synthesis and Structural Properties of Niobium Pentoxide Powders: A Comparative Study of the Growth Process. *Materials Research*, *19*(6), 1381–1387. https://doi.org/10.1590/1980-5373-mr-2015-0733

[23]. Gu, Z., Li, K., Wang, H., Wei, Y., Yan, D., & Qiao, T. (2013). Syngas production from methane over CeO2-Fe2O3 mixed oxides using a chemical-looping method. *Kinetics and Catalysis*, *54*(3), 326–333. https://doi.org/10.1134/S002315841303004X

[24]. Genovese, N. A., Gorlani, A., & Arroyo P, A. H. (2005). GTL Technology and It's Role in The World Energy Markets. Master Medea, Scuola Mattei,.